Analytical energy gradients of a self-consistent reaction-field solvation model based on CM2 atomic charges

Tianhai Zhu and Jiabo LiDaniel A. LiotardChristopher J. Cramer and Donald G. Truhlar

Citation: The Journal of Chemical Physics **110**, 5503 (1999); doi: 10.1063/1.478447
View online: http://dx.doi.org/10.1063/1.478447
View Table of Contents: http://aip.scitation.org/toc/jcp/110/12
Published by the American Institute of Physics

Analytical energy gradients of a self-consistent reaction-field solvation model based on CM2 atomic charges

Tianhai Zhu and Jiabo Li
Department of Chemistry and Supercomputer Institute, University of Minnesota, Minneapolis, Minnesota 55455-0431

Daniel A. Liotard
Laboratoire de Physico-Chimie Théorique, Université de Bordeaux 1, 351 Cours de la Liberation, 33405 Talence Cedex, France

Christopher J. Cramer and Donald G. Truhlar
Department of Chemistry and Supercomputer Institute, University of Minnesota, Minneapolis, Minnesota 55455-0431

(Received 20 November 1998; accepted 15 December 1998)

Analytical energy gradients have been derived for an SM5-type solvation model based on Hartree–Fock self-consistent reaction-field theory and CM2 atomic charges. The method is combined with an analytic treatment of the first derivatives of nonelectrostatic first-solvation-shell contributions to the free energy and implemented in the General Atomic and Molecular Electronic Structure System (GAMESS). The resulting equations allow one to use accurate class IV charges to calculate equilibrium geometries of solutes in liquid-phase solutions. The algorithm is illustrated by calculations of optimized geometries and solvation free energies for water, methanol, dimethyl disulfide, and 9-methyladenine in water and 1-octanol. © *1999 American Institute of Physics.* [S0021-9606(99)30311-1]

I. INTRODUCTION

The use of continuum models to calculate solvation effects has, despite its relative simplicity, become a very useful tool for studying solvent effects.[1–3] In particular, the SM5.42R solvation model,[4–6] which is based on fixed solute geometries and is the newest and most advanced member of the SM*x* suite of solvation models,[7–17] yields solvation free energies accurate to better than 0.5 kcal/mol for typical organic solutes in both water and organic solvents. The SM5.42R solvation model has a number of key features. First, it takes into account the mutual solute–solvent electric polarization by a variational self-consistent reaction-field (SCRF) approach based on the generalized Born (GB) approximation[1,2,18,19] with the highly accurate Charge Model 2 (CM2).[20] Second, it includes nonelectrostatic first-solvation-shell effects by parameterized, geometry-dependent and solvent-property-dependent atomic surface tensions. This approach not only allows a straightforward calculation of the solvation contributions to the Fock matrix, but also was designed to make it possible to obtain analytical energy gradients, which are crucial for accurate and efficient geometry optimizations. The present paper presents the formalism for such energy gradients.

Our earlier solvation models,[7–17] SM1–SM5.4, were based on semi-empirical molecular orbital theory, and they included geometry optimization for SM1–SM4 and for SM5.4. For SM1–SM4, geometry optimization has been carried out based on energy gradients obtained by finite differences, and for SM5.4 it is based on analytic free energy gradients implemented in version 6.1 of the AMSOL code.[21] The electrostatic component of Solvation Model 5.4[11–14,16] is based on the CM1[22] class IV charge model, which provides gas-phase dipole moments with a root-mean-square error (RMSE) of 0.26–0.30 D for 195 neutral molecules based on wave functions calculated by semi-empirical molecular orbital theory with the neglect of diatomic differential overlap. In order to provide comparable or better accuracy for dipole moments calculated from *ab initio* Hartree–Fock (HF) theory,[23,24] density functional theory[25] (DFT), or hybrid Hartree–Fock density-functional theory[26,27] (HF-DFT) calculations, where it is essential to retain overlap effects, we developed the CM2[20] class IV charge model, which is based on Löwdin charges[28] including overlap. This procedure, with an appropriate choice of basis set, can yield gas-phase dipole moments with an RMSE of 0.19 D for HF theory and DFT and 0.18 D for HF-DFT, as measured by a test set of 211 neutral compounds. Furthermore, the CM2 mapping procedure gives slightly improved results (RMSE about 0.03 D lower when compared for the same set of 185 neutral compounds) even for semiempirical molecular orbital theory, showing that it provides a more balanced procedure even in that limit. Solvation model SM5.42R[4–6] is based on these improved charges and is parameterized for DFT,[4–6] HF,[5,6] HF-DFT,[6] and semi-empirical molecular orbital theory.[6] The model was parameterized with ''rigid'' gas-phase geometries (meaning that the geometries were not relaxed in solution), and this is indicated by the ''R'' at the end of the model name. The present paper contains the theory required to use this model without the R, i.e., with geometry optimization in liquid-phase solutions. This should give more accurate geometries and partial charges in liquid-phase solutions, although—since the atomic surface tensions are not reparam-

eterized with geometry optimization—absolute solvation energies may be slightly too negative on the average.

Analytic energy gradients for gas-phase calculations were pioneered by Bratoz,[29] Gerratt and Mills,[30] and Pulay,[31,32] and there have been several extensions, in addition to the one[21] mentioned above, to include the electrostatic component of free energy gradients in the liquid phase. For example, analytic first and second free energy derivatives have been derived for the conductorlike screening model[33] (COSMO) and implemented with HF theory, second-order Møller–Plesset perturbation theory, and DFT.[34] Calculations of analytic free energy gradients and solution geometry optimizations have also been reported with the Dmol/COSMO model.[35] Rinaldi and co-workers presented the analytic expressions for the first and second derivatives of the Hartree–Fock energy in the case of a solvated system simulated by a multipolar charge distribution embedded in an ellipsoid,[36] and Dillet and co-workers extended this to a cavity of arbitrary shape.[37] Tomasi and co-workers have presented analytic derivative formulas for the polarized continuum model based on an integral equation formulation.[38] By combining any of these treatments[21,33–38] with the derivatives of the exposed surface areas and the atomic surface tensions,[21,39,40] one can include first-solvation-shell effects in the geometry optimization. However, none of these treatments is general enough to include CM2 charges as required for an SM5.42 model.

In this paper, we present our work to extend the SM5.42 solvation approach to include analytic free energy gradients and geometry optimizations in solution. The implementation is demonstrated in the General Atomic and Molecular Electronic Structure System[41] (GAMESS) at the Hartree–Fock level and is illustrated by optimizing geometries and computing solvation free energies for several polar solutes in water and 1-octanol.

II. ANALYTIC FREE ENERGY GRADIENTS

A deviation of the analytic gradient of the free energy of solvation is presented in Appendix A. Here we present a brief summary with emphasis on the aspects that are new.

For simplicity, we here consider a solution consisting of a closed-shell solute molecule with N nuclei in a continuous medium that has a dielectric constant ϵ. In the SMx solvation approach with the restricted Hartree–Fock approximation[23] and n basis functions for the electronic orbitals of the solute, the standard-state free energy G_S^0 of the solute with a fixed geometry in the liquid phase is given by

$$G_S^0 = E_{EN} + G_P + G_{\mathrm{CDS}}, \tag{1a}$$

where

$$E_{EN} = \frac{1}{2}\sum_{rs}^{n} P_{rs}^{(1)}(h_{rs} + F_{rs}^{(0)}) + \sum_{b<c}^{N} \frac{Z_b Z_c}{|\mathbf{R}_b - \mathbf{R}_c|}, \tag{1b}$$

where r and s are indices of atomic basis functions, $\mathbf{P}^{(1)}$ is the density matrix optimized in the presence of solvent, $\mathbf{h}$ and $\mathbf{F}^{(0)}$ are matrix representations of the usual one-electron and Fock operators in the absence of solvent, and Z_b and Z_c are nuclear charges for atoms b and c. Thus, E_{EN} is the ground-state solute electronic internal energy and nuclear repulsion computed for the wave function corresponding to $\mathbf{P}^{(1)}$, G_P is the gain in electric polarization energy due to the mutual polarization of the solvent and solute, and G_{CDS} is the first-solvation-shell contribution to free energy of solvation, including inter alia, cavitation, dispersion, and specific solvent structural changes (CDS) in the first solvation shell. Note that for Eq. (1b), $\mathbf{F}^{(0)}$ is computed from the liquid-phase density matrix $\mathbf{P}^{(1)}$. This liquid-phase matrix representation of the gas-phase Fock operator differs from the gas-phase matrix representation of the gas-phase Fock operator because the self-consistent field changes when the orbitals relax in solution.

Since G_S^0 is calculated by a method that is variationally optimized with respect to the density matrix,[4–6] the gradient of G_S^0 with respect to the solute atomic position $\mathbf{R}_a$ of atom a is given by

$$\begin{aligned}\frac{\partial G_S^0}{\partial \mathbf{R}_a} = &\sum_{rs}^{n} P_{rs}^{(1)} \left\langle r \left| \frac{\partial \hat{h}}{\partial \mathbf{R}_a} \right| s \right\rangle + \frac{\partial E_N}{\partial \mathbf{R}_a} + 2\sum_{rs}^{n} P_{rs}^{(1)} \langle r^a | \hat{h} | s \rangle \\ &+ 2\sum_{rstv}^{n} P_{rs}^{(1)} P_{tv}^{(1)} \left[(r^a s | tv) - \frac{1}{2}(r^a t | sv) \right] \\ &- \sum_{rs}^{n} W_{rs}^{(1)} \left(\frac{\partial S_{rs}}{\partial \mathbf{R}_a} \right) + \left(\frac{\partial G_P}{\partial \mathbf{R}_a} \right)_{\mathbf{P}^{(1)}} + \frac{\partial G_{\mathrm{CDS}}}{\partial \mathbf{R}_a},\end{aligned} \tag{2}$$

where t and v are indices of atomic basis functions, E_N is the nuclear repulsion energy given by the last summation of Eq. (1b), $\mathbf{W}^{(1)}$ is the energy-weighted density matrix in the presence of solvent, $\mathbf{S}$ is the overlap matrix,

$$\langle r^a | \hat{h} | s \rangle = \left\langle \frac{\partial \chi_r}{\partial \mathbf{R}_a} | \hat{h} | \chi_s \right\rangle, \tag{3}$$

$$(r^a s | tv) = \left\langle \frac{\partial \chi_r(1)}{\partial \mathbf{R}_a} \chi_s(1) \left| \frac{1}{r_{12}} \right| \chi_t(2) \chi_v(2) \right\rangle, \tag{4}$$

where χ_r, χ_s, χ_t, and χ_v are basis functions, and r^a denotes the derivative of the basis function χ_r centered on atom a with respect to $\mathbf{R}_a$. The first two terms in Eq. (2) give the Hellmann–Feynman electrostatic contribution; the third and fourth terms are called the integral force; and the term that involves the energy-weighted density matrix is the so-called density force or Pulay force.[31,32] The integral force term contains the derivatives of the basis functions, which are defined in Eqs. (3) and (4).

In the GB approximation,[1,2,18,19,42,43] G_P is computed as

$$G_P = -\frac{1}{2}\left(1 - \frac{1}{\epsilon}\right) \sum_{bc}^{N} q_b q_c \gamma_{bc}, \tag{5}$$

where q_b and q_c are atomic charges on atoms b and c, and γ_{bc} is the Coulomb integral between b and c given by[43]

$$\gamma_{bc} = \frac{1}{\sqrt{|\mathbf{R}_b - \mathbf{R}_c|^2 + \alpha_b \alpha_c [\exp(-|\mathbf{R}_b - \mathbf{R}_c|^2 / d_{bc} \alpha_b \alpha_c)]}}, \tag{6}$$

where α_b and α_c are the effective Born radii for atoms b and c, and d_{bc} is a parameter. The partial derivative $(\partial G_P/\partial \mathbf{R}_a)_{\mathbf{P}^{(1)}}$ is computed using the expression

$$\left(\frac{\partial G_P}{\partial \mathbf{R}_a}\right)_{\mathbf{P}^{(1)}} = -\frac{1}{2}\left(1-\frac{1}{\epsilon}\right)\sum_{b=1}^{N}\sum_{c=1}^{N}\left[2q_c\gamma_{bc}\left(\frac{\partial q_b}{\partial \mathbf{R}_a}\right)_{\mathbf{P}^{(1)}} + q_b q_c\left(\frac{\partial \gamma_{bc}}{\partial \mathbf{R}_a}\right)\right]. \tag{7}$$

The effective Born radii are functions of the exposed surface areas of all solute atoms.[43] They are computed using the force trapezoid algorithm[39] with analytical evaluation of exposed surface areas.[39] The term $\partial\gamma_{bc}/\partial\mathbf{R}_a$ contains the derivatives of the exposed surface areas of atoms a and b with respect to $\mathbf{R}_a$. These derivatives are carried out analytically[21,40] using the ASA algorithm,[39] as implemented previously in AMSOL 6.1[21] and are discussed further in Sec. III B. If the CM2 charge model is employed, then

$$\left(\frac{\partial q_b}{\partial \mathbf{R}_a}\right)_{\mathbf{P}^{(1)}} = -\sum_{r\in b}\left(\frac{\partial \mathbf{S}^{1/2}}{\partial \mathbf{R}_a}\mathbf{P}^{(1)}\mathbf{S}^{1/2} + \mathbf{S}^{1/2}\mathbf{P}^{(1)}\frac{\partial \mathbf{S}^{1/2}}{\partial \mathbf{R}_a}\right)_{rr} + \sum_{c\neq b}\sum_{r\in b}\sum_{r\in c}\left[\left(\mathbf{P}^{(1)}\frac{\partial \mathbf{S}}{\partial \mathbf{R}_a}\right)_{rs}(\mathbf{P}^{(1)}\mathbf{S})_{sr} + (\mathbf{P}^{(1)}\mathbf{S})_{rs}\left(\mathbf{P}^{(1)}\frac{\partial \mathbf{S}}{\partial \mathbf{R}_a}\right)_{sr}\right](D_{bc}+2C_{bc}B_{bc}), \tag{8}$$

where D_{bc} and C_{bc} are CM2 parameters, and B_{bc} is Mayer's bond order[44] between atoms b and c. Notice that the derivative in Eq. (8) is defined to be taken with $\mathbf{P}^{(1)}$ fixed.

The G_{CDS} term and its derivatives are computed as follows

$$G_{\mathrm{CDS}} = \sum_b^N \sigma_b^A A_b + \sigma^M \sum_b^N A_b, \tag{9}$$

$$\frac{\partial G_{\mathrm{CDS}}}{\partial \mathbf{R}_a} = \sum_b\left[\frac{\partial \sigma_b^A}{\partial \mathbf{R}_a}A_b + (\sigma_b^A+\sigma^M)\frac{\partial A_b}{\partial \mathbf{R}_a}\right], \tag{10}$$

where σ_b^A is the atomic-number-dependent and possibly geometry-dependent contribution to the atomic surface tension of atom b, σ^M is a contribution to the surface tension which does not depend on atomic numbers or solute geometry, and A_b is the exposed surface area of atom b, whose derivative with respect to $\mathbf{R}_a$ is again evaluated analytically using the ASA scheme.[21,39,40] The functional forms for the geometry- and atomic-number-dependent atomic surface tensions in SM5.42R are specified in previous articles.[4,17]

The derivatives in Eq. (10) of the atomic surface tension contributions with respect to solute nuclear coordinates along with a full derivation of Eqs. (1)–(8) are given in Appendix A.

III. IMPLEMENTATION

III. A. Derivative of $S^{1/2}$

All the terms in the total energy gradient expression given in Eq. (2) are straightforward to compute except the partial derivative of G_P. To evaluate this term based on Eqs. (7) and (8), we need to obtain the derivatives of $\mathbf{S}^{1/2}$ with respect to nuclear positions. The problem of computing $\partial\mathbf{S}^{1/2}/\partial\mathbf{R}_a$ would be greatly simplified if the two matrices, $\partial\mathbf{S}^{1/2}/\partial\mathbf{R}_a$ and $\mathbf{S}^{1/2}$, were to commute. However, we found that in general they do not commute. Thus we implemented the following approach. We start with the equality

$$\mathbf{S}^{1/2}\mathbf{S}^{1/2} = \mathbf{S}. \tag{11}$$

Taking derivatives on both sides with respect to $\mathbf{R}_a$ gives

$$\frac{\partial \mathbf{S}^{1/2}}{\partial \mathbf{R}^a}\mathbf{S}^{1/2} + \mathbf{S}^{1/2}\frac{\partial \mathbf{S}^{1/2}}{\partial \mathbf{R}^a} = \frac{\partial \mathbf{S}}{\partial \mathbf{R}^a}. \tag{12}$$

Let $\mathbf{X}\equiv\partial\mathbf{S}^{1/2}/\partial\mathbf{R}_a$, $\mathbf{A}\equiv\mathbf{S}^{1/2}$, and $\mathbf{B}\equiv\partial\mathbf{S}/\partial\mathbf{R}_a$, so that Eq. (12) becomes

$$\mathbf{XA}+\mathbf{AX}=\mathbf{B}. \tag{13}$$

This is the well-known matrix form of the Lyapunov equation. One of the most effective methods of solving Eq. (13) for $\mathbf{X}$ is the Bartels–Stewart algorithm,[45] which is based on the Schur reduction to triangular form by an orthogonal similarity transformation. It is a stable $O(n^3)$ algorithm, with n being the order of $\mathbf{A}$ (recall that n is the number of basis functions). An alternative algorithm is presented in Appendix B.

III. B. Derivatives of exposed surface areas

The derivative $\partial\gamma_{bc}/\partial\mathbf{R}_d$ that occurs in Eq. (7) also requires further discussion. First of all we note from Eq. (6) that the only difficult part of this derivative is evaluation of the derivatives $\partial\alpha_b/\partial\mathbf{R}_d$ of the effective Coulomb radii. The effective Coulomb radius is given by[7,39,43]

$$\alpha_b = \left[\int_{\rho_b}^{R'}\frac{dr}{r^2}f(r) + \frac{1}{R'}\right]^{-1}, \tag{14}$$

where $f(r)$ is the fractional exposed area

$$f = \frac{A_b(r)}{4\pi r^2} \tag{15}$$

in which $A_b(r)$ is the exposed area of a sphere of radius r centered at the nucleus of atom b. The exposed area is the area not buried inside any of the other atoms k of the solute when they are represented by spheres of radius ρ_k, where ρ_k is the ''intrinsic Coulomb radius'' of atom k. Let R be the value of r at which the sphere on atom b engulfs all the other spheres. Equation (14) is correct provided that $R'\geq R$. In our previous work we have set $R'=R$.

To evaluate $\partial\alpha_b/\partial\mathbf{R}_d$, we use the relation

$$\frac{\partial \alpha_b}{\partial \mathbf{R}_d} = -\alpha_b^2\int_{\rho_b}^{R'}\frac{dr}{r^2}\frac{\partial f(r)}{\partial \mathbf{R}_d} \tag{16}$$

which is valid if all ρ_k are constants, which is indeed the case in the SM5.42 model. Using the ASA formulation,[39] the integrand of (16) may be evaluated analytically from derivatives of direction cosines, dot products, vector products, and inverse trigonometric functions.

Our previous implementation[21] of analytic gradients for SM5.4 was exact provided there are no N–H or O–H bonds

in the solute. The inexactness in the latter case arises because in SM5.4, the intrinsic Coulomb radius of H depends on solute geometry if the H atom is within 2 Å of an N or O atom. Thus the gradient of Eq. (7) includes partial derivatives $\partial\rho_b/\partial\mathbf{R}_b$ (when $d=b$), and $\partial\rho_k/\partial\mathbf{R}_d$ (for other atoms k). The latter contribution was included only for the atom k' that determines the upper bound R of the integration. The neglected contributions are only the ones coming from H atoms with a nonconstant intrinsic Coulomb radius that are neither atom b nor k' for a given α_b. This missing contribution was checked carefully by comparison to numerical gradients, and it is usually of minor (negligible) importance. Nevertheless, one improvement of SM5.42 as compared to SM5.4 is that all intrinsic Coulomb radii are now taken as constants, and this completely eliminates these small but complicated terms.

The success of the procedure used here depends on the accuracy and numerical smoothness of the radial quadrature in Eq. (14). We have considered two methods for carrying out this quadrature, namely the force trapezoid (FT) algorithm presented previously[39] and a new algorithm, called the force Gauss–Legendre (FGL) algorithm, which is discussed next. The main motivation for the introduction of the FGL algorithm is that the FT algorithm leads to a small but systematic overestimate of the integral. This is because $f(r)$ is approximated locally by a linear function, whereas the actual $f(r)$ for typical molecular geometries is concave, i.e., it usually has a positive second derivative for low values of r, which are weighted the most heavily by the r^{-2} factor in the integrand.

A second issue of concern regarding the FT algorithm concerns the number M of integration steps used between ρ_b and R. One could have unstable gradient calculations if the algorithm for determining M allowed M to increase and decrease with fluctuations in R as the geometry changes. To circumvent this in a geometry optimization run, we allow M to increase but never to decrease; thus fluctuations are avoided. The AMSOL code[21] also has an option to freeze M at any constant, pre-selected value.

In principle, by increasing M until the FT algorithm is completely converged, both the deviation of the integrand from local linearity and the nonsmoothness of the approximant due to increasing M can be made vanishingly small. We have found, however, that systematic errors and nonsmoothness can be reduced more efficiently by changing to a Gauss–Legendre scheme in a new independent variable x defined by

$$x=\ln r. \tag{17}$$

Then

$$\alpha_b=\left[\int_{\ln\rho_b}^{\ln R}\frac{dx}{x}\exp[f(e^x)]+\frac{1}{R}\right]^{-1}. \tag{18}$$

It turns out that $f(e^x)/x$ is very well approximated by low- and medium-order polynomials, so the Gauss–Legendre quadrature of the integral in Eq. (18) works very well. Furthermore the number M of points in the integration that are required for a given accuracy depends more on the number N of atoms in the solute than on its geometry. The following empirical rule works very well:

$$M=\min\begin{cases}\mathrm{INT}(t_1+t_2N)\\ 16\end{cases}, \tag{19}$$

where t_1 and t_2 are constants depending on the desired accuracy, and the INT function truncates a real number to an integer.

We tested the accuracy and cost of various choices of t_1 and t_2 for the solvation free energy of a sample set of 10 solutes (with the maximum value of N being 76 and average value of N being 28.2). The results are in the L^∞ section of Table I. (The norm column is explained below.) The $t_1=7$, $t_2=0.09$ case in Table I would be a good compromise of accuracy and efficiency for semi-empirical methods since the computer round-off in semi-empirical packages easily reaches 0.2 kcal/mol for molecules with 50 atoms. The choice of $t_1=14$, $t_2=0.07$ would provide an efficient scheme for more precise work, which is desired for use with *ab initio* and DFT packages.

In practice the cost of *ab initio* and DFT calculations is dominated by SCF cycling, not by this quadrature. Thus one may increase the cost of the quadrature without having a major impact on the overall cost. Indeed one might wish to use some overkill, especially if Hessians are to be calculated by finite differences of gradients, if geometries are to be optimized, or if reaction paths are to be calculated in regions where the free energy surface is approximately flat, since these types of calculations are very sensitive to small numerical noise in the energies and gradients. Nevertheless it is of interest to consider the accuracy attained with smaller values of t_1 and t_2 in order to demonstrate the intrinsic accuracies of the alternative quadrature schemes.

Finally we return to the question of the choice of R'. The choice made so far, $R'=R$, has the advantage that it confines the numerical quadrature to the smallest possible region where analytic integration is impossible. But the disadvantage is that R has discontinuous partial derivatives with respect to the geometry of the solute.

TABLE I. Tests of radial quadrature schemes.

				Error (cal/mol)			
Norm	Method	t_1	t_2	MS[a]	RMS[b]	MA[c]	Cost[d]
L^∞	FT[e]	–	–	16	39	67	11.8
	FGL	16	0	−1	6	16	14.2
		14	0.07	2	5	11	13.4
		12	0.07	−2	14	31	11.8
		7	0.09	−11	24	64	7.8
		4	0.05	−36	91	184	3.8
L^{36}	FT[e]	–	–	18	38	92	11.7
	FGL	10	0.20	0.3	19	49	13.3

[a]Mean signed (a measure of the bias).
[b]Root mean square.
[c]Maximum absolute (worst case).
[d]Average value of M.
[e]With default parameters of AMSOL package–version 6.1 (Ref. 21); namely, first integration step 0.15 Å, and each succeeding step larger by a factor of 1.2.

Let r_k be the distance from atom b to atom k. Similarly let

$$R_k = r_k + \rho_k . \tag{20}$$

Then

$$R = \max_{k \neq b} R_k . \tag{21}$$

If we consider the R_k values as the components of a vector of length $N-1$, then

$$R = \|R_k\|_\infty , \tag{22}$$

where the L^p norm is defined by

$$\|R_k\|_p = \left[\sum_{k=1}^{N-1} |R_k| p \right]^{1/p} .$$

The source of the discontinuous derivatives of R is the choice of $p = \infty$. Any finite, even value of p would lead to a smooth function. Furthermore

$$\|R_k\|_p \geqslant \|R_k\|_\infty .$$

Therefore, the counterintuitive but mathematically natural solution to our problem is to adopt an L^p norm (with p a positive, even number) to prescribe the upper limit to the integration. After some trial and error we selected the L^{36} norm as being ''near enough'' to the L^∞ result, but smooth. (On older machines or some PCs where numbers greater than 10^{38} cause overflow, one might choose smaller p for large molecules.)

For the L^{36} norm we carried out a series of tests on a sample of 31 molecules, with N covering the range 2–76 rather uniformly. The results are in the last two rows of Table I. Again the results with FGL are better than those with FT. Since the cost of this step is not a major component of the overall cost, the most significant aspect of the new algorithm is the reduced spread of errors and greater smoothness. In separate tests we have shown that this leads to much more symmetrical structures for geometry optimization of molecules with symmetry and to much more accurate vibrational frequencies. For example, for the vibrational frequencies of methane, the FGL scheme with $M = 11$ yields an rms error of less than 0.2 cm^{-1}, with deviations up to 0.06 cm^{-1} between frequencies that should be equivalent by symmetry, whereas the FT scheme with our previous default parameters and the L^∞ norm yields an rms error of 12 cm^{-1} with differences of up to 13 cm^{-1} between frequencies that should be equivalent by symmetry. (In all cases, errors are computed relative to a converged trapezoidal integration with a step size of 0.005 Å.)

III. C. Incorporation in GAMESS

Using the methods described above, we have implemented analytic free energy gradients in the GAMESOL 2.0 module,[46] which is a package for adding solvation to GAMESS.[41] (The current version of GAMESOL obtains $\partial \mathbf{S}^{1/2}/\partial \mathbf{R}_a$ by the Bartels–Stewart algorithm and evaluates γ_{bc} and $\partial \gamma_{bc}/\partial \mathbf{R}_a$ by the FT algorithm with the L^∞ norm, although the tests presented here indicate it would be worthwhile to switch in a later version to the FGL algorithm with the L^{36} norm for the upper limit of integration.) GAMESOL 2.0 contains a module called `smx`, which can be added to GAMESS for SM5.42R and SM5.42 solvation calculations. GAMESOL 2.0 also contains three modified GAMESS modules, `rhfuhf`, `grdl`, and `mthlib`, that are needed in order to incorporate `smx` into GAMESS.

IV. DISCUSSION

The present scheme for analytical derivatives was designed to yield gradients that are smooth functions of geometry, which is a requirement for robust geometry optimizations and calculations of Hessians and reaction paths. This is possible because of several design features in the SM5.42 solvation model. First of all, the dependence of surface tensions on bond orders, which was used in SM2–SM4, has been replaced in SM5 models by a direct dependence on geometry, using functional forms with an infinite number of continuous derivatives. Second, the dependence of Coulomb radii on partial charge (as employed in SM1–SM4) or on geometry (as employed in SM5.4) has also been removed, so all Coulomb radii are constants. Finally by means of the generalized Born approximation, the electrostatic calculation has been reduced to a radial quadrature over an integrand that depends on geometry-dependent analytical surface areas with analytical derivatives. Smooth results can be obtained from the radial quadrature by a force trapezoid algorithm with a sufficiently small step size or by a force Gauss–Legendre quadrature in the logarithmic metric with L^{36} calculation of the upper bound for integration.

Methods like COSMO[33,34] or PCM,[38] which use 2-D discretization techniques instead of analytic surface areas to solve the electrostatic problem, cannot yield gradients as smooth as the present algorithm. The Rinaldi–Rivail model[36,37] could be made smooth, but this has not been fully implemented.

As an example of the difficulties with 2-D discretization schemes, consider the algorithm used for COSMO.[33] The cavity is built from ''segments'' of nearly equal areas, where each segment is attached to an atom. The model must satisfy rotational invariance. Therefore the spatial location of the segments attached to an atom a is based on a local Cartesian frame which is centered on the atom a and is defined from three other atoms (b, c, and d) chosen near a. This defines a rotation matrix $\mathbf{Q}$ from the laboratory frame to the local frame on a. The precise location of each segment on a is determined from an iterative procedure to place a regular polyhedron centered on a and oriented according to $\mathbf{Q}$. This procedure ''P'' also yields the area for each segment of a. The analytical expression for the molecular gradient is easy to compute if and only if one neglects the effects of the changes both in $\mathbf{Q}$ and in P. In the original implementation,[33] changes in P were neglected, and changes in $\mathbf{Q}$ were made to be zero by the way that the rotation matrices were built. The latter choice introduces a hysteresis into the number and spatial location of the segments and, as a consequence, into the solvation free energy. In the AMPAC–version 6.0 package[47] the hysteresis was removed (as required for using many optimizers), but the contributions from changes in $\mathbf{Q}$ were still

TABLE II. Selected optimized geometrical parameters using SM5.42/HF/MIDI!6D for (A) water in water, (B) methanol in water, and (C) dimethyl disulfide in 1-octanol. Gas-phase HF/MIDI!6D and HF/MIDI! geometrical parameters are listed for comparison. Bond lengths are in Å, and bond angles are in degrees.

	Solution MIDI!6D ISCRF=1[a]	Solution MIDI!6D ISCRF=2[b]	Gas MIDI!6D	Gas MIDI!
Water in water				
O–H	0.972	0.972	0.967	0.967
HOH	100.6	100.6	102.4	102.6
Methanol in water				
O–H	0.970	0.970	0.967	0.946
O–C	1.426	1.429	1.424	1.400
HOC	106.0	105.5	106.6	109.3
Dimethyl disulfide in 1-octanol				
S–S	2.123	2.123	2.121	2.118
S–C	1.831	1.830	1.831	1.833
SSC	97.7	97.6	97.4	97.3

[a]ISCRF=1 denotes the full treatment explained in the text.
[b]ISCRF=2 denotes a treatment in which the gas-phase bond orders are used to calculate the charge modification term q_a^C [see Eq. (A22)] of the CM2 charge model.

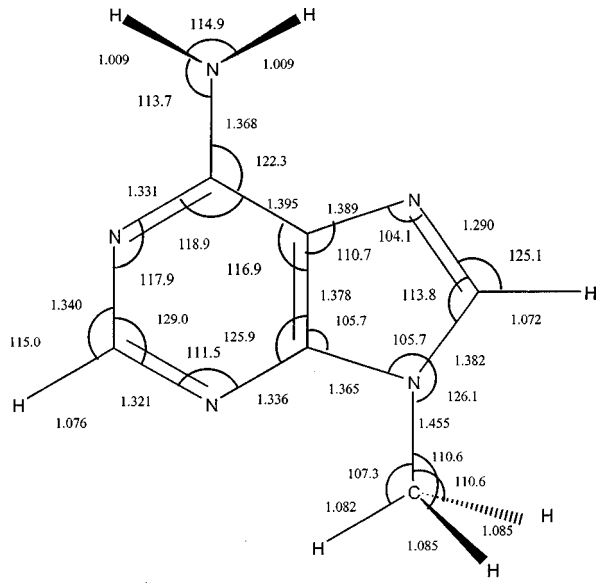

FIG. 1. Optimized structure of 9-methyladenine in the gas phase at the HF/MIDI!6D level. Distances are in angstroms, and angles are in degrees. Only one distance and three angles change in the first four significant figures when the basis is changed from MIDI! to MIDI!6D, namely, the C(6)–N(amino) distance from 1.368 to 1.367, the C(3)–N(3)–C(4) angle from 111.5 to 111.6, the N(3)–C(4)–C(5) angle from 125.9 to 125.8, and the C(6)–N(1)–C(2) angle from 117.9 to 117.8.

neglected. We mention these kinds of difficulties simply to motivate a better appreciation for the present algorithm, which does not have these difficulties. The present algorithm is smooth in principle, and in practice simply requires sufficient care with the radial quadratures.

Another advantage of the present algorithm is that the generalized Born approximation,[2,18,19,42,43] like the multipole expansion algorithm,[3,36,37] does not suffer from the outlying charge error[1,48,49] of methods[33–35,38] based on the apparent charge distribution induced on a cavity surface.

V. TEST CALCULATIONS

We present sample calculations based on the SM5.42R solvation model with the HF/MIDI!6D parametrization as implemented in GAMESOL 2.0. The MIDI!6D basis is identical to the MIDI! basis presented elsewhere[50,51] except that five-function spherical harmonic *d* subshells are replaced by six-function Cartesian *d* subshells (which also contain one *s* function). We have optimized solution geometries and computed solvation free energies for (A) water in water, (B) methanol in water, (C) dimethyl disulfide in 1-octanol, and (D) 9-methyladenine in water. In all calculations, gas-phase HF/MIDI! solute geometries were taken as initial structures. The geometries were optimized in the liquid phase until the absolute value of the largest gradient component was less than 0.0005 atomic units.

Table II lists some selected optimized liquid-solution SM5.42/HF/MIDI!6D geometrical parameters for systems A, B, and C, and it compares then with their gas-phase HF/MIDI!6D and HF/MIDI! analogs. For a given basis (MIDI!6D), we found that the O–H bond in water and the S–S bond in dimethyl disulfide are stretched by 0.005 Å and 0.002 Å, respectively, and the O–H and O–C bonds in methanol are lengthened by 0.003 and 0.005 Å, respectively, and the bond angles change by 0.12–1.8 degrees. The changes for CH_3OH and $(CH_3S)_2$ are smaller than the change in geometry in passing from MIDI! to MIDI!6D in the gas phase, whereas for water in water the changes are larger. Note that the O–H bond of methanol lengthens upon solvation, similar to the effect in water, to expose the hydroxylic proton more to solvent. The H–O–H and C–O–H bond angles narrow, which is reasonable when the O–H bond lengthens (less *s* character on O is associated with longer bonds and narrower angles). In water, because of the narrower bond angle, solvation shortens the H–H distance from 1.507 Å to 1.496 Å, bringing the positively charged centers closer (their repulsion is partially shielded by solvent, and bringing atoms of similar charge together concentrates the charge and thereby increases the solvation energy). Thus the trends are rational.

Figure 1 shows the optimized structure of 9-methyladenine in water using the SM5.42/HF/MIDI!6D basis set. Comparing to the gas-phase HF/MIDI! geometry, shown in Fig. 2, we again found most of the bond lengths increase while bond angles decrease. But the changes are small and they only bring down the solvation free energy by 0.3 kcal/mol (from −13.7 kcal/mol at the gas-phase HF/MIDI! geometry to −14.0 kcal/mol at the optimized solution geometry). To show that the differences between Figs. 1 and 2 are primarily due to solvation rather than basis set, the caption for Fig. 1 lists the only geometrical parameters given in Fig. 1 that change in the first four significant figures when the basis is changed from MIDI! to MIDI!6D. We see that the solvation effects are much larger.

The fairly small change in solvation free energy upon

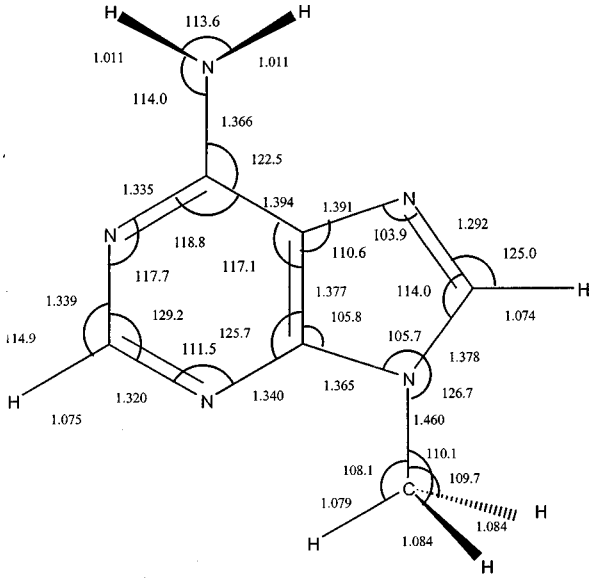

FIG. 2. Optimized structure of 9-methyladenine in water at SM5.42/HF/MIDI!6D level.

geometry optimization computed at the SM5.42/HF/MIDI! level is entirely consistent with results from earlier SM*x* models. For instance, the SM2.1/AM1 and SM5.4/AM1 levels of theory predict geometry relaxation to contribute only -0.39 and -0.41 kcal/mol, respectively, to the solvation free energy of 9-methyladenine. An earlier analysis of the five most common nucleic acid bases, both methylated and unmethylated, at the SM2/AM1 level[52] concluded that the primary effect of geometric relaxation was to permit increased charge separation in molecules already possessing significant electric moments. As 9-methyladenine has relatively little charge separation, as judged by its small dipole moment (roughly 3.0 D in solution, depending on the level of theory), geometric relaxation has only a marginal effect. Obviously this will not necessarily be the case for systems where soft normal modes are coupled with large degrees of charge separation—transition-state structures in particular might be expected to have such a characteristic—and geometry optimization may be of particular interest for such systems.

VI. CONCLUDING REMARKS

We have derived analytical energy gradients for self-consistent reaction-field calculations based on charges obtained by the CM2 class IV charge model. The result is general enough to be used with semi-empirical molecular orbital theory, *ab initio* Hartree–Fock theory, density functional theory, or hybrid Hartree–Fock density-functional theory. It is illustrated by implementing it for SM5.42 calculations of geometries and free energies of solvation in liquid-phase solutions. The calculations are carried out by *ab initio* Hartree–Fock theory in the GAMESS package. The method yields accurate and efficient geometry optimizations for liquid-phase solutions, and in the future these gradients should also be useful for calculating the equilibrium solvation path[53,54] for chemical reactions in solution.

ACKNOWLEDGMENTS

The authors are grateful to Gregory D. Hawkins and Paul Winget for helpful assistance. This work was in part supported by the National Science Foundation (grant CHE97-25965), the U.S. Army Research Office, and also by the National Institute of Standards and Technology through the general computational methodology provisions of an Advanced Technology Project subcontract with Phillips Petroleum Company.

APPENDIX A: DERIVATION OF ANALYTICAL GRADIENTS FOR THE SM5.42 SOLVATION MODEL

We consider a solute with N nuclei in a continuous medium with a dielectric constant ϵ. The continuous medium represents an ideal (i.e., infinitely dilute) liquid-phase solution. In the SM*x* approach,[2,4–14,16] the standard-state free energy of the solution, G_S^0, is partitioned into two terms:

$$G_S^0 = G_{ENP} + G_{\mathrm{CDS}}, \tag{A1}$$

where G_{ENP} includes the SCF solute electronic (E) energy and nuclear (N) repulsion and the solute-solvent polarization (P) energy, and G_{CDS} is the free energy of solvation due to first-solvation-shell effects such as cavitation, dispersion, and solvent structural changes (CDS). The electrostatic term, G_{ENP}, can be written

$$G_{ENP} = E_{EN} + G_P, \tag{A2}$$

where E_{EN} is the ground-state electronic energy and nuclear repulsion of the distorted solute, and G_P is the free energy of electric polarization energy due to the mutual polarization of the solvent and solute. Note that E_{EN} is an internal energy term for the solute as distorted by the presence of the solvent, and G_P includes not only the solute-solvent interaction terms (which are net favorable) but also the free energy cost of polarizing the solvent. The gradient of G_S^0 with respect to atomic position $\mathbf{R}_a$ of atom a is

$$\frac{\partial G_S^0}{\partial \mathbf{R}_a} = \frac{\partial E_{EN}}{\partial \mathbf{R}_a} + \frac{\partial G_P}{\partial \mathbf{R}_a} + \frac{\partial G_{\mathrm{CDS}}}{\partial \mathbf{R}_a}. \tag{A3}$$

In the restricted Hartree–Fock approximation, E_{EN} can be written

$$E_{EN} = E_E + E_N = \frac{1}{2}\sum_{rs}^{n} P_{rs}^{(1)}(h_{rs} + F_{rs}^{(0)}) + \sum_{a<b}^{N} \frac{Z_a Z_b}{|\mathbf{R}_a - \mathbf{R}_b|}, \tag{A4}$$

where r and s are indices of atomic basis functions, n is the number of basis functions, $\mathbf{P}^{(1)}$ is the electronic density matrix in the presence of solvent, $\mathbf{h}$ and $\mathbf{F}^{(0)}$ are the matrix representations of the usual one-electron and gas-phase Fock operators, and Z_a and Z_b are nuclear charges for atoms a and b. We further note that $\mathbf{P}^{(1)}$, $\mathbf{h}$, and $\mathbf{F}^{(0)}$ are defined as:

$$P_{rs}^{(1)} = 2\sum_{i=1}^{N/2} C_{ir}^{(1)} C_{is}^{(1)}, \tag{A5}$$

$$h_{rs} = \langle \chi_r | \hat{h} | \chi_s \rangle, \tag{A6}$$

$$F_{rs}^{(0)} = h_{rs} + \sum_{tv}^{n} P_{tv}^{(1)} \left[(rs|tv) - \frac{1}{2}(rt|sv) \right], \tag{A7}$$

$$(rs|tv)=\left\langle \chi_r(1)\chi_s(1)\left|\frac{1}{r_{12}}\right|\chi_t(2)\chi_v(2)\right\rangle, \tag{A8}$$

where t and v are indices of atomic basis functions, $\{C_{ir}^{(1)}\}$ are molecular orbital coefficients for orbital i in the presence of solvent, and χ_r, χ_s, χ_t, and χ_v are atomic basis functions. Note in particular that $\mathbf{F}^{(0)}$ is evaluated using $\mathbf{P}^{(1)}$, not using the gas-phase density matrix. In the SM*x* solvation approach, G_P is calculated by the generalized Born formula:[1,2,18,19,42,43]

$$G_P=-\frac{1}{2}\left(1-\frac{1}{\epsilon}\right)\sum_{ab}^{N} q_a q_b \gamma_{ab}, \tag{A9}$$

where q_a and q_b are atomic charges on atoms a and b, and γ_{ab} is the Coulomb integral between atoms a and b given by

$$\gamma_{ab}=\frac{1}{\sqrt{|\mathbf{R}_a-\mathbf{R}_b|^2+\alpha_a\alpha_b[\exp(-|\mathbf{R}_a-\mathbf{R}_b|^2/d_{ab}\alpha_a\alpha_b)]}}, \tag{A10}$$

where d_{ab} is a constant, and α_a and α_b are effective radii which depend on a set of parameterized Coulomb radii.[7] Although we use ϵ for the dielectric constant in Eq. (A9) and for orbital eigenvalues elsewhere, no confusion should result since the dielectric constant always appears as a reciprocal, and the orbital eigenvalues never do. Furthermore, the orbital eigenvalues $\epsilon_i^{(0)}$ and $\epsilon_i^{(1)}$ have superscripts, (0) and (1), denoting gas-phase or solution, respectively. When shown in bold, $\boldsymbol{\epsilon}^{(1)}$ is the diagonal matrix with $\epsilon_i^{(1)}$ as the diagonal elements.

Before proceeding we define a shorthand notation for the derivatives of the basis functions, namely,

$$\langle r^a|\hat{h}|s\rangle=\left\langle \frac{\partial\chi_r}{\partial\mathbf{R}_a}\left|\hat{h}\right|\chi_s\right\rangle, \tag{A11}$$

$$(r^a s|tv)=\left\langle \frac{\partial\chi_r(1)}{\partial\mathbf{R}_a}\chi_s(1)\left|\frac{1}{r_{12}}\right|\chi_t(2)\chi_v(2)\right\rangle, \tag{A12}$$

where r^a denotes the derivative of a basis function χ_r centered on atom a with respect to $\mathbf{R}_a$. In the derivation below we shall take account of symmetry relations that follow from these definitions, i.e., $(r^a s|tv)=(sr^a|tv)=(tv|r^a s)=(tv|sr^a)$.

We stress that the SM*x* solvation approach is based on self-consistent reaction field (SCRF) theory,[1–3] which means that the solute atomic charges depend on the solution density matrix, and both of them are iterated to self-consistency. Taking the derivative of Eqs. (A3) and (A9) with respect to $\mathbf{R}_a$, we have (after simplification)

$$\begin{aligned}\frac{\partial G_{ENP}}{\partial\mathbf{R}_a}=&\sum_{rs}^{n} P_{rs}^{(1)}\left\langle r\left|\frac{\partial\hat{h}}{\partial\mathbf{R}_a}\right|s\right\rangle+\sum_{b\neq a}^{N} Z_a Z_b\frac{\mathbf{R}_a-\mathbf{R}_b}{|\mathbf{R}_a-\mathbf{R}_b|^3}\\&+2\sum_{rs}^{n} P_{rs}^{(1)}\langle r^a|\hat{h}|s\rangle+2\sum_{rstv}^{n} P_{rs}^{(1)}P_{tv}^{(1)}\left[(r^a s|tv)\right.\\&\left.-\frac{1}{2}(r^a t|sv)\right]+\sum_{ir}\frac{\partial G_{ENP}}{\partial C_{ir}^{(1)}}\frac{\partial C_{ir}^{(1)}}{\partial\mathbf{R}_a}\\&+\left(\frac{\partial G_P}{\partial\mathbf{R}_a}\right)_{\mathbf{P}^{(1)}}.\end{aligned} \tag{A13}$$

The first two terms in Eq. (A11) give the Hellmann–Feynman electrostatic contribution; the third and fourth terms are called the integral force.[31] The integral force terms contain the derivatives of the basis functions defined in Eqs. (A11) and (A12). The fifth term, which involves the derivatives of molecular orbital coefficients, seems to present a difficult problem since molecular orbital coefficients do not depend on the solute nuclear positions explicitly. Fortunately, as shown by Pulay,[31] we do not need these derivatives to evaluate this term. The key is that for the solute to be in its ground state, G_{ENP} should be stationary with respect to the molecular orbital coefficients $\mathbf{C}^{(1)}$ under the following orthonormality condition:

$$[\mathbf{C}^{(1)}]^{\dagger}\mathbf{S}\mathbf{C}^{(1)}=\mathbf{I}_n, \tag{A14}$$

where $\mathbf{S}$ is the overlap matrix, and $\mathbf{I}_n$ is the $n\times n$ unit matrix. Using the Lagrangian constraint minimization, we have

$$\frac{\partial}{\partial C_{ir}^{(1)}}\{G_{ENP}-\mathrm{Tr}(\boldsymbol{\epsilon}^{(1)}([\mathbf{C}^{(1)}]^{\dagger}\mathbf{S}\mathbf{C}^{(1)}-\mathbf{I}_n))\}=0 \tag{A15}$$

and

$$\frac{\partial G_{ENP}}{\partial C_{ir}^{(1)}}=2(\mathbf{S}\mathbf{C}^{(1)}\boldsymbol{\epsilon}^{(1)})_{ir}. \tag{A16}$$

The fifth term in Eq. (A11) now becomes

$$\begin{aligned}\sum_{ir}\frac{\partial G_{ENP}}{\partial C_{ir}^{(1)}}\frac{\partial C_{ir}^{(1)}}{\partial\mathbf{R}_a}&=2\sum_{ir}(\mathbf{S}\mathbf{C}^{(1)}\boldsymbol{\epsilon}^{(1)})_{ir}[C_{ir}^{(1)}]^a\\&=2\,\mathrm{Tr}(\mathbf{S}\mathbf{C}^{(1)}\boldsymbol{\epsilon}^{(1)}[\mathbf{C}^{(1)}]^{a\dagger}),\end{aligned} \tag{A17}$$

where the superscript a means taking the derivative with respect to $\mathbf{R}_a$. If we differentiate the orthonormality condition in Eq. (A14), we have

$$[\mathbf{C}^{(1)}]^{a\dagger}\mathbf{S}\mathbf{C}^{(1)}+[\mathbf{C}^{(1)}]^{\dagger}\mathbf{S}[\mathbf{C}^{(1)}]^a=-[\mathbf{C}^{(1)}]^{\dagger}[\mathbf{S}]^a\mathbf{C}^{(1)}. \tag{A18}$$

Multiplying Eq. (A18) by the matrix $\boldsymbol{\epsilon}^{(1)}$ and taking the trace we obtain

$$\begin{aligned}2\,\mathrm{Tr}(\mathbf{S}\mathbf{C}^{(1)}\boldsymbol{\epsilon}^{(1)}[\mathbf{C}^{(1)}]^{a\dagger})&=-\mathrm{Tr}(\mathbf{C}^{(1)}\boldsymbol{\epsilon}^{(1)}[\mathbf{C}^{(1)}]^{\dagger}[\mathbf{S}]^a)\\&=-\mathrm{Tr}(\mathbf{W}^{(1)}[\mathbf{S}]^a),\end{aligned} \tag{A19}$$

where the energy-weighted density matrix $\mathbf{W}^{(1)}=\mathbf{C}^{(1)}\boldsymbol{\epsilon}^{(1)}\times[\mathbf{C}^{(1)}]^{\dagger}$ is introduced. Equation (A17) now can be written

$$\sum_{ir}\frac{\partial G_{ENP}}{\partial C_{ir}^{(1)}}\frac{\partial C_{ir}^{(1)}}{\partial\mathbf{R}_a}=-\sum_{rs}^{N_b} W_{rs}^{(1)}\left(\frac{\partial S_{rs}}{\partial\mathbf{R}_a}\right) \tag{A20}$$

and is called the density force or Pulay force.[31]

The last term in Eq. (A11) is the partial derivative of G_P with respect to $\mathbf{R}_a$ for a fixed solute density matrix. Note that although G_P itself depends on the solution density matrix (through solute atomic charges), we do not need to work out explicitly the terms containing the derivatives of the molecular orbital coefficients with respect to nuclear positions in $\partial G_P/\partial\mathbf{R}_a$ because these terms are already included in the density force term. From Eq. (A9), we obtain

$$\left(\frac{\partial G_P}{\partial \mathbf{R}_a}\right)_{\mathbf{P}^{(1)}} = -\frac{1}{2}\left(1-\frac{1}{\epsilon}\right)\sum_{a=1}^{N}\sum_{b=1}^{N}\left[2q_b\gamma_{ab}\left(\frac{\partial q_a}{\partial \mathbf{R}_a}\right)_{\mathbf{P}^{(1)}} + q_a q_b\left(\frac{\partial \gamma_{ab}}{\partial \mathbf{R}_a}\right)\right]. \tag{A21}$$

The term $\partial\gamma_{ab}/\partial\mathbf{R}_a$ contains the derivatives of the exposed surface areas of atoms a and b with respect to $\mathbf{R}_a$.[21,39,40] If the CM2 charge model is employed, as in SM5.42 models, we have

$$q_a = q_a^L + q_a^C = q_a^L + \sum_{b\neq a}^{N} B_{ab}(D_{ab}+C_{ab}B_{ab}), \tag{A22}$$

where q_a is the CM2 charge on atom a, q_a^L is the atomic charge obtained from Löwdin population analysis, q_a^C is the CM2 correction term to the Löwdin charge q_a^L, D_{ab} and C_{ab} are CM2 parameters, and B_{ab} is Mayer's bond order[42] between atoms a and b. Note that q_a^L and B_{ab} are given by

$$q_a^L = Z_a - \sum_{r\in a}(\mathbf{S}^{1/2}\mathbf{P}^{(1)}\mathbf{S}^{1/2})_{rr}, \tag{A23}$$

$$B_{ab} = \sum_{r\in a}\sum_{s\in b}(\mathbf{P}^{(1)}\mathbf{S})_{rs}(\mathbf{P}^{(1)}\mathbf{S})_{sr}. \tag{A24}$$

This gives

$$\left(\frac{\partial q_a}{\partial \mathbf{R}_a}\right)_{\mathbf{P}^{(1)}} = -\sum_{r\in a}\left(\frac{\partial \mathbf{S}^{1/2}}{\partial \mathbf{R}_a}\mathbf{P}^{(1)}\mathbf{S}^{1/2} + \mathbf{S}^{1/2}\mathbf{P}^{(1)}\frac{\partial \mathbf{S}^{1/2}}{\partial \mathbf{R}_a}\right)_{rr} + \sum_{b\neq a}\left[\sum_{r\in a}\sum_{s\in b}\left(\mathbf{P}^{(1)}\frac{\partial \mathbf{S}}{\partial \mathbf{R}_a}\right)_{rs}(\mathbf{P}^{(1)}\mathbf{S})_{sr} + (\mathbf{P}^{(1)}\mathbf{S})_{rs}\left(\mathbf{P}^{(1)}\frac{\partial \mathbf{S}}{\partial \mathbf{R}_a}\right)_{sr}\right](D_{ab}+2C_{ab}B_{ab}). \tag{A25}$$

In SM5-type solvation models, the CDS term is computed as

$$G_{\mathrm{CDS}} = \sum_a \sigma_a^A A_a + \sigma^M \sum_a A_a = \sum_a (\sigma_a^A + \sigma^M)A_a, \tag{A26}$$

where σ_a^A is the contribution to the atomic surface tension of atom a that depends on the atomic number of a and possibly on the solute geometry, σ^M is the contribution which does not depend on atomic numbers or geometry, and A_a is the exposed surface area of atom a.[2,4–17] In practice the constant σ^M can be absorbed into the function σ_a^A when that is convenient. It follows from Eq. (A26) that

$$\frac{\partial G_{\mathrm{CDS}}}{\partial \mathbf{R}_a} = \sum_a\left[\frac{\partial \sigma_a^A}{\partial \mathbf{R}_a}A_a + (\sigma_a^A+\sigma^M)\frac{\partial A_a}{\partial \mathbf{R}_a}\right], \tag{A27}$$

where the derivative $\partial A_a/\partial\mathbf{R}_a$ is evaluated as before.[21,39,40] The rest of this Appendix presents the derivatives of σ_a^A with respect to solute nuclear coordinates.

The functional forms for the geometry- and atomic-number-dependent atomic surface tensions in SM5.42R are specified in a previous paper.[4] They all involve a cutoff tanh function, which we call a COT, and which is defined as

$$T_{ab} \equiv T(R_{ab}) \equiv \begin{cases} \exp\left[-\dfrac{\Delta R}{\Delta R + \bar{R} - R_{ab}}\right] & R_{ab} \leqslant \bar{R} + \Delta R \\ 0 \quad \text{otherwise} \end{cases}, \tag{A28}$$

where R_{ab} is the distance between atoms a and b, and ΔR and $\bar{R}$ are constant parameters. (As explained in previous papers, ΔR and $\bar{R}$ may and do have different values in different COTs, but it is unnecessary to complicate our notation to show this fact since each derivative of a COT may be evaluated individually.) Let X_a be the x coordinate for atom a centered at $\mathbf{R}_a$, then

$$\frac{\partial T_{ab}}{\partial X_a} = \frac{dT_{ab}}{dR_{ab}}\frac{\partial R_{ab}}{\partial X_a} = \frac{dT_{ab}}{dR_{ab}}\frac{X_a - X_b}{R_{ab}}, \tag{A29}$$

$$\frac{\partial T_{ab}}{\partial X_b} = \frac{dT_{ab}}{dR_{ab}}\frac{\partial R_{ab}}{\partial X_b} = \frac{dT_{ab}}{dR_{ab}}\frac{X_b - X_a}{R_{ab}}, \tag{A30}$$

where

$$\frac{dT_{ab}}{dR_{ab}} = -T_{ab}\frac{\Delta R}{(\Delta R + \bar{R} - R_{ab})^2}. \tag{A31}$$

The SM5.42R atomic surface tension functional forms[4,17] can be divided into five types. We next give the derivatives of σ_a^A for each type, in each case reducing the result to a function involving the elementary derivatives (A29) and (A30). We note that all sums over b should be interpreted to have the restriction $b\neq a$, and all sums over c should be interpreted to have the restrictions $c\neq b$ and $c\neq a$. Thus the atoms labeled a, b, and c come from mutually exclusive sets. Furthermore b' is another atom from the set of atoms labeled b, and similarly c' is from the c set. As a consequence we also have $b'\neq a$, $c'\neq a$, $c'\neq b$, and $c'\neq b'$. Furthermore, although a, b, c, b', and c' denote individual atoms, A, B, and C are just labels on surface tension coefficients. (Recall that σ_a^A, T_{ab}, T_{bc}, etc. are functions, whereas $\tilde{\sigma}_A$, $\tilde{\sigma}_{AB}$, etc. are constants, called surface tension coefficients.)

Type I:

$$\sigma_a^A = \tilde{\sigma}_A + \tilde{\sigma}_{AB}\sum_b T_{ab}, \tag{A32}$$

$$\frac{\partial \sigma_a^A}{\partial X_a} = \tilde{\sigma}_{AB}\sum_b \frac{\partial T_{ab}}{\partial X_a}, \tag{A33}$$

$$\frac{\partial \sigma_a^A}{\partial X_b} = \tilde{\sigma}_{AB}\frac{\partial T_{ab}}{\partial X_b}, \tag{A34}$$

Type II:

$$\sigma_a^A = \tilde{\sigma}_A + \tilde{\sigma}_{ABC}\sum_b T_{ab}\sum_c T_{bc}, \tag{A35}$$

$$\frac{\partial \sigma_a^A}{\partial X_a} = \tilde{\sigma}_{ABC}\sum_b \frac{\partial T_{ab}}{\partial X_a}\sum_c T_{bc}, \tag{A36}$$

$$\frac{\partial \sigma_a^A}{\partial X_b} = \tilde{\sigma}_{ABC} \frac{\partial T_{ab}}{\partial X_b} \sum_c T_{bc} + \tilde{\sigma}_{ABC} T_{ab} \sum_c \frac{\partial T_{bc}}{\partial X_b}, \tag{A37}$$

$$\frac{\partial \sigma_a^A}{\partial X_c} = \tilde{\sigma}_{ABC} \sum_b T_{ab} \frac{\partial T_{bc}}{\partial X_c}; \tag{A38}$$

Type III:

$$\sigma_a^A = \tilde{\sigma}_A + \tilde{\sigma}_{AB} \left(\sum_b T_{ab} \right)^2, \tag{A39}$$

$$\frac{\partial \sigma_a^A}{\partial X_a} = 2 \tilde{\sigma}_{AB} \sum_b T_{ab} \sum_{b'} \frac{\partial T_{ab'}}{\partial X_a}, \tag{A40}$$

$$\frac{\partial \sigma_a^A}{\partial X_b} = 2 \tilde{\sigma}_{AB} \frac{\partial T_{ab}}{\partial X_b} \sum_{b'} T_{ab'}; \tag{A41}$$

Type IV:

$$\sigma_a^A = \tilde{\sigma}_A + \tilde{\sigma}_{AB} \left\{ \sum_b \left[T_{ab} \left(\sum_b T_{bc} \right)^2 \right] \right\}^{1.3}, \tag{A42}$$

$$\frac{\partial \sigma_a^A}{\partial X_a} = 1.3 \tilde{\sigma}_{AB} \left\{ \sum_b \left[T_{ab} \left(\sum_c T_{bc} \right)^2 \right] \right\}^{0.3} \times \sum_{b'} \frac{\partial T_{ab'}}{\partial X_a} \left(\sum_{c'} T_{b'c'} \right)^2, \tag{A43}$$

$$\frac{\partial \sigma_a^A}{\partial X_b} = 1.3 \tilde{\sigma}_{AB} \left\{ \sum_{b'} \left[T_{ab'} \left(\sum_c T_{bc} \right)^2 \right] \right\}^{0.3} \times \left[\frac{\partial T_{ab}}{\partial X_b} \left(\sum_{c'} T_{bc'} \right)^2 + 2 T_{ab} \sum_{c''} T_{bc''} \sum_{c'''} \frac{\partial T_{bc'''}}{\partial X_b} \right], \tag{A44}$$

$$\frac{\partial \sigma_a^A}{\partial X_c} = 2.6 \tilde{\sigma}_{AB} \left\{ \sum_b \left[T_{ab} \left(\sum_{c'} T_{bc'} \right)^2 \right] \right\}^{0.3} \times \sum_{b'} T_{ab'} T_{b'c} \frac{\partial T_{b'c}}{\partial X_c}; \tag{A45}$$

Type V:

$$\sigma_a^A = \tilde{\sigma}_A + \tilde{\sigma}_{AB} T(T_a), \tag{A46}$$

$$T_a = -\sum_b T_{ab} \tag{A47}$$

$$\frac{\partial \sigma_a^A}{\partial X_a} = -\tilde{\sigma}_{AB} \frac{dT}{dT_a} \sum_b \frac{\partial T_{ab}}{\partial X_a}, \tag{A48}$$

$$\frac{\partial \sigma_a^A}{\partial X_b} = -\tilde{\sigma}_{AB} \frac{dT}{dT_a} \frac{\partial T_{ab}}{\partial X_b}. \tag{A49}$$

APPENDIX B

Although we found that the Bartels–Stewart algorithm is very satisfactory for solving Eq. (13), this method ignores the fact that the eigenvalues and eigenvectors of **S** are already known because they are required to compute $\mathbf{S}^{1/2}$. We therefore present another algorithm which might be useful for future work.

Since **S** is positive definite, we may write its eigenvalues as $\mathbf{V}^2$, with **V** real. Again letting $\mathbf{A} \equiv \mathbf{S}^{1/2}$, and letting **C** denote the matrix of orthonormal eigenvectors, we have

$$\mathbf{AC} = \mathbf{CV} \tag{B1}$$

and

$$\mathbf{A} = \mathbf{CVC}^T, \tag{B2}$$

where *T* denotes a transpose. Left multiplying Eq. (13) by $\mathbf{C}^T$ and right multiplying by **C** yields

$$\mathbf{YV} + \mathbf{VY} = \mathbf{R}, \tag{B3}$$

where

$$\mathbf{Y} = \mathbf{C}^T \mathbf{X} \mathbf{C} \tag{B4}$$

and

$$\mathbf{R} = \mathbf{C}^T \mathbf{B} \mathbf{C}. \tag{B5}$$

Since **V** is diagonal and square,

$$Y_{ij} = Y_{ji} = \frac{R_{ij}}{V_{ii} + V_{jj}}. \tag{B6}$$

Then

$$\mathbf{X} = \mathbf{CYC}^T. \tag{B7}$$

This scheme for computing **X**, like the one in Sec. III, is $O(n^3)$, but it is dominated by matrix operations that can be coded and executed very efficiently, so it may be worth trying. However, we note that the cost of this step is not a major component of the computational effort. In fact, the cost of geometry optimizations in solution is not much larger than the cost of gas-phase geometry optimizations with the present method.

[1] J. Tomasi and M. Persico, Chem. Rev. **94**, 2027 (1994).
[2] C. J. Cramer and D. G. Truhlar, in *Reviews in Computational Chemistry*, edited by D. B. Boyd and K. B. Lipkowitz (VCH, New York, 1995), Vol. 6, p. 1.
[3] J.-L. Rivail and D. Rinaldi, in *Computational Chemistry: Reviews of Current Trends*, edited by J. Leszczynski (World Scientific, Singapore, 1996), Vol. 1, p. 139.
[4] T. Zhu, J. Li, G. D. Hawkins, C. J. Cramer and D. G. Truhlar, J. Chem. Phys. **109**, 9117 (1998).
[5] J. Li, G. D. Hawkins, C. J. Cramer, and D. G. Truhlar, Chem. Phys. Lett. **288**, 293 (1998).
[6] J. Li, T. Zhu, G. D. Hawkins, P. Winget, D. A. Liotard, C. J. Cramer, and D. G. Truhlar, Theor. Chem. Acc. (in press).
[7] C. J. Cramer and D. G. Truhlar, J. Am. Chem. Soc. **113**, 8305 (1991).
[8] C. J. Cramer and D. G. Truhlar, Science **256**, 213 (1992).
[9] C. J. Cramer and D. G. Truhlar, J. Comput. Chem. **13**, 1089 (1992).
[10] D. J. Giesen, J. W. Storer, C. J. Cramer, and D. G. Truhlar, J. Am. Chem. Soc. **117**, 1057 (1995).
[11] C. C. Chambers, G. D. Hawkins, C. J. Cramer, and D. G. Truhlar, J. Phys. Chem. **100**, 16385 (1996).
[12] G. D. Hawkins, C. J. Cramer, and D. G. Truhlar, J. Phys. Chem. **100**, 19824 (1996).
[13] D. J. Giesen, M. Z. Gu, C. J. Cramer, and D. G. Truhlar, J. Org. Chem. **61**, 8720 (1996).
[14] D. J. Giesen, C. C. Chambers, C. J. Cramer, and D. G. Truhlar, J. Phys. Chem. B **101**, 2061 (1997).
[15] (a) G. D. Hawkins, C. J. Cramer, and D. G. Truhlar, J. Phys. Chem. B **101**,

7147 (1997); (b) G. D. Hawkins, D. A. Liotard, C. J. Cramer, and D. G. Truhlar, J. Org. Chem. **63**, 4305 (1998).
[16] D. J. Giesen, G. D. Hawkins, D. A. Liotard, C. J. Cramer, and D. G. Truhlar, Theor. Chem. Acc. **98**, 85 (1997).
[17] G. D. Hawkins, C. J. Cramer, and D. G. Truhlar, J. Phys. Chem. B **102**, 3257 (1998).
[18] I. Jano, Compt. Rend. Acad. Sci. (Paris) **261**, 103 (1965).
[19] O. Tapia, in *Quantum Theory of Chemical Reactions*, edited by R. Daudel, A. Pullman, L. Salem, and A. Viellard (Reidel, Dordrecht, 1980), Vol. 2, p. 25.
[20] J. Li, T. Zhu, C. J. Cramer, and D. G. Truhlar, J. Phys. Chem. A **102**, 1820 (1998).
[21] G. D. Hawkins, D. J. Giesen, C. C. Chambers, G. C. Lynch, I. Rossi, J. W. Storer, D. Rinaldi, D. A. Liotard, C. J. Cramer, and D. G. Truhlar, AMSOL–version 6.1, University of Minnesota, Minneapolis, 1997.
[22] J. W. Storer, D. J. Giesen, C. J. Cramer, and D. G. Truhlar, J. Computer-Aided Mol. Des. **9**, 87 (1995).
[23] C. C. J. Roothaan, Rev. Mod. Phys. **23**, 69 (1951).
[24] W. J. Hehre, L. Radom, P. v. R. Schleyer, and J. A. Pople, *Ab Initio Molecular Orbital Theory* (Wiley, New York, 1986).
[25] *Density Functional Theory of Molecules, Clusters, and Solids*, edited by D. E. Ellis (Kluwer, Dordrecht, 1995).
[26] A. D. Becke, J. Chem. Phys. **98**, 1372 (1993).
[27] P. J. Stephens, F. J. Devlin, C. S. Ashwar, K. L. Bak, P. R. Taylor, and M. J. Frisch, ACS Symp. Ser. **629**, 105 (1996).
[28] P.-O. Löwdin, J. Chem. Phys. **18**, 365 (1950).
[29] S. Bratoz, Colloques Internationaux du Centre Natl. Rech. Sci. (Paris) **82**, 287 (1958).
[30] J. Gerratt and I. M. Mills, J. Chem. Phys. **49**, 1719 (1968).
[31] P. Pulay, in *Modern Theoretical Chemistry*, edited by H. F. Schaefer III (Plenum, New York, 1977), Vol. 4, p. 153.
[32] P. Pulay, Mol. Phys. **17**, 197 (1969).
[33] A. Klamt and G. Schüürmann, J. Chem. Soc., Perkin Trans. 2, 799 (1993).
[34] T. N. Truong and E. V. Stefanovich, J. Chem. Phys. **103**, 3709 (1995).
[35] J. Andzelm and C. Kolmel, J. Chem. Phys. **103**, 9312 (1995).
[36] D. Rinaldi, J.-L. Rivail, and N. Rguini, J. Comput. Chem. **13**, 675 (1992).
[37] V. Dillet, D. Rinaldi, J. Bertrán, J. Rivail, J. Chem. Phys. **104**, 9437 (1996).
[38] (a) M. Cossi, J. Tomasi, and R. Cammi, Int. J. Quantum Chem., Symp. **29**, 695 (1995); (b) V. Barone, M. Cossi, and J. Tomasi, J. Comput. Chem. **19**, 404 (1998); (c) E. Cances, B. Menucci, and J. Tomasi, J. Chem. Phys. **109**, 260 (1998).
[39] D. A. Liotard, G. D. Hawkins, G. C. Lynch, C. J. Cramer, and D. G. Truhlar, J. Comput. Chem. **16**, 422 (1995).
[40] I. Tuñon, J. Bertrán, M. F. Ruiz-Lopez, and D. Rinaldi, J. Comput. Chem. **17**, 148 (1996).
[41] M. W. Schmidt, K. K. Baldridge, J. A. Boatz, S. T. Elbert, M. S. Gordon, J. H. Jensen, S. Koseki, N. Matsunaaga, K. A. Nguyen, S. J. Su, T. L. Windus, M. Dupuis, and J. A. Montgomery, J. Comput. Chem. **14**, 1347 (1993).
[42] S. C. Tucker and D. G. Truhlar, Chem. Phys. Lett. **157**, 164 (1987).
[43] W. C. Still, A. Tempczyk, R. C. Hawley, and T. Hendrickson, J. Am. Chem. Soc. **112**, 6127 (1990).
[44] I. Mayer, Chem. Phys. Lett. **97**, 270 (1983).
[45] R. H. Bartels and G. W. Stewart, Commun. ACM **15**, 820 (1972).
[46] J. Li, T. Zhu, G. D. Hawkins, D. Rinaldi, D. A. Liotard, C. J. Cramer, and D. G. Truhlar, GAMESOL–version 2.0, University of Minnesota, Minneapolis, October 1998.
[47] AMPAC–version 6.0, Semichem, Inc., Shawnee Mission, KS, 1997.
[48] K. Baldridge and A. Klamt, J. Chem. Phys. **106**, 6622 (1997).
[49] (a) B. Menucci and J. Tomasi, J. Chem. Phys. **106**, 5151 (1997); (b) M. Cossi, B. Menucci, J. Pitarch, and J. Tomasi, J. Comput. Chem. **19**, 833 (1998).
[50] R. E. Easton, D. J. Giesen, A. Welch, C. J. Cramer, and D. G. Truhlar, Theor. Chim. Acta **93**, 281 (1996).
[51] J. Li, C. J. Cramer, and D. G. Truhlar, Theor. Chem. Acc. **99**, 192 (1998).
[52] C. J. Cramer and D. G. Truhlar, Chem. Phys. Lett. **198**, 74 (1992); Chem. Phys. Lett. **202**, 567(E) (1993).
[53] S. C. Tucker and D. G. Truhlar, J. Am. Chem. Soc. **112**, 3347 (1990).
[54] Y.-Y. Chuang, C. J. Cramer, and D. G. Truhlar, Int. J. Quantum Chem. **70**, 887 (1998).